



**EUROfusion**

WP17ER-PR(17) 18369

V. V. Baran et al.

## **Trapped electron mode turbulence: test mode approach**

Preprint of Paper to be submitted for publication in  
Romanian Journal of Physics



This work has been carried out within the framework of the EUROfusion Consortium and has received funding from the Euratom research and training programme 2014-2018 under grant agreement No 633053. The views and opinions expressed herein do not necessarily reflect those of the European Commission.

This document is intended for publication in the open literature. It is made available on the clear understanding that it may not be further circulated and extracts or references may not be published prior to publication of the original when applicable, or without the consent of the Publications Officer, EUROfusion Programme Management Unit, Culham Science Centre, Abingdon, Oxon, OX14 3DB, UK or e-mail [Publications.Officer@euro-fusion.org](mailto:Publications.Officer@euro-fusion.org)

Enquiries about Copyright and reproduction should be addressed to the Publications Officer, EUROfusion Programme Management Unit, Culham Science Centre, Abingdon, Oxon, OX14 3DB, UK or e-mail [Publications.Officer@euro-fusion.org](mailto:Publications.Officer@euro-fusion.org)

The contents of this preprint and all other EUROfusion Preprints, Reports and Conference Papers are available to view online free at <http://www.euro-fusionscipub.org>. This site has full search facilities and e-mail alert options. In the JET specific papers the diagrams contained within the PDFs on this site are hyperlinked

1 TRAPPED ELECTRON MODE TURBULENCE: TEST MODES APPROACH

2 V. V. BĂRAN<sup>1,2,a</sup>, D. PALADE<sup>1,2</sup>, M. VLAD<sup>1</sup>, F. SPINEANU<sup>1</sup>

3 <sup>1</sup>National Institute for Laser, Plasma and Radiation Physics, Str. Atomistilor, Nr. 409, PO Box  
4 MG-36, 077125 Magurele, Bucharest Romania

5 <sup>2</sup>Faculty of Physics, University of Bucharest, Str. Atomistilor, Nr. 405, PO Box MG-11, 077125,  
6 Magurele, Bucharest Romania

7 *E-mail*<sup>a</sup>: virgil.baran@inflpr.ro

8 *Received July 27, 2017*

9 *Abstract.* We perform a test mode analysis for the case of the dissipative TEM  
10 instability in slab geometry, by studying the influence of the statistical properties of a  
11 turbulent background on the frequencies and growth rates of the test modes. Our ap-  
12 proach naturally incorporates the ion trajectory diffusion and ion stochastic trapping  
13 present already in the quasilinear and, respectively, weakly nonlinear stages of the tur-  
14 bulence evolution.

15 *Key words:* Trapped electron modes, turbulence evolution, test modes.

16

17 *PACS:* 52.35.Ra, 05.10.Gg, 05.40.-a

## 1. INTRODUCTION

18 The understanding of turbulence evolution in tokamak plasmas is a very active  
19 topic in both theoretical and experimental fusion research. In magnetically confined  
20 plasmas, the particle and heat transport is strongly influenced by the low frequency  
21 drift type turbulence, driven by the gradients of the temperature, density, magnetic  
22 field, etc. The most relevant drift instabilities are the ion temperature gradient (ITG),  
23 the electron temperature gradient (ETG) and the dissipative and collisionless trapped  
24 electron modes (DTEM and CTEM) [1–6].

25 In this work, we will limit ourselves to the study of the trapped electron modes.  
26 DTEMs are caused by a strong temperature gradient and large collisionality, being  
27 associated with the edge of the tokamak, while CTEMs are generated by the electron  
28 curvature drift resonance, being relevant in the core [7]. In the context of tokamak  
29 plasma experiments, TEMs play an important role in advanced confinement regimes  
30 with electron transport barriers and in the hot electron regime, relevant for experi-  
31 ments with dominant central electron heating (see Ref. [8] and references therein).

32 We present a study of DTEMs in turbulent plasma that is focused on the ef-  
33 fect of trajectory trapping in the structure of the background turbulence. The latter  
34 is due to the stochastic particle advection caused by the electric drift, which leads

35 to trajectory eddying. The statistics of trajectories may strongly deviate from Gaus-  
 36 sianity in the presence of trapping. We follow the philosophy of [12, 14]: starting  
 37 from the drift kinetic equations, we obtain a dispersion relation for test modes which  
 38 is dependent on the statistical properties of the background turbulence. In turn, the  
 39 frequencies and growth rates of the test modes will provide the tendencies of the  
 40 turbulence evolution.

41 In the first Section we discuss the electron and ion responses to a perturbation  
 42 of the potential for the DTEM case, in a drift kinetic framework. In Section 2, we will  
 43 analyze the resulting dispersion relation for the test modes, and in the final Section  
 44 we will discuss the results.

## 2. TEM-SLAB

45 The basic physical mechanisms of the DTEM instability may be evidenced  
 46 even in the absence of the complexities inherent to the toroidal geometry. Indeed,  
 47 the simplest setup in which the instability manifests itself consists of an essentially  
 48 straight magnetic field, supplemented by two localised magnetic mirrors ensuring the  
 49 population of trapped electrons [9, 10].

50 Our model consists of a low  $\beta$  plane plasma slab. The magnetic field is di-  
 51 rected along the  $z$  axis, i.e.  $\mathbf{B} = B\mathbf{e}_z$ , and the plasma nonuniformity is considered  
 52 along the  $x$  axis, i.e.  $n_0 = n_0(x)$ ,  $T_e = T_e(x)$ . The characteristic density and temper-  
 53 ature lengths,  $L_n = n_0 |dn_0/dx|^{-1}$  and  $L_{T_e} = T_e |dT_e/dx|^{-1}$  are much larger than  
 54 the wavelengths of the drift modes. At  $z = \pm L$ , there are two well localized, per-  
 55 fectly reflecting magnetic mirrors which confine a fraction  $\delta < 1$  of the total electron  
 56 population. The untrapped electrons and ions are allowed to flow in the whole plasma  
 57 volume, extending between  $z = \pm L'$ .

58 We start from the gyrokinetic equations for electrons and ions in the case of a  
 59 Larmor radius smaller than the correlation length of the potential:

$$60 \quad \partial_t f^\alpha - \frac{\nabla\phi \times \mathbf{b}}{B} \cdot \nabla f^\alpha + v_z \partial_z f^\alpha - \frac{q_\alpha}{m_\alpha} \partial_z \phi \frac{\partial}{\partial v_z} f^\alpha = \mathcal{C}^\alpha, \quad (1)$$

61 where  $\alpha = e, i$ ,  $\phi$  being the potential of the turbulence and  $\mathcal{C}^\alpha$  the collision term.  
 62 Here, we consider characteristic wavelengths larger than the ion Larmor radius, lead-  
 63 ing to negligible effects when averaging the potential over the gyromotion. In the  
 64 following, we consider a background potential  $\phi_0$  and study test modes on the turbu-  
 65 lent plasma.

### 2.1. SHORT TIME EQUILIBRIUM

66 In order to study the electron and ion responses to a test mode in a turbulent  
 67 background potential, we need to evaluate the deviations from an equilibrium distri-

68 bution function, even if the latter is valid only for a short time.

69 In the case of the electrons the parallel dynamics dominates, and the last two  
70 terms in (1) are much larger than the first two terms. The electron solution of (1)  
71 for short time (smaller than the characteristic times of the first two terms) may be  
72 obtained by neglecting them:

$$73 \quad f_0^e = n_0(x) F_M^e \exp\left(\frac{e\phi_0}{T_e}\right), \quad F_M^e = \left(\frac{m_e}{2\pi T_e}\right)^{3/2} \exp\left(-\frac{m_e \mathbf{v}^2}{2T_e}\right), \quad (2)$$

74 where  $e = |e|$  and  $F_M^e$  is the Maxwell distribution of the electron velocities.

75 In the case of the ions, the perpendicular dynamics is dominant, and the last two  
76 terms in Eq. (1), corresponding to large characteristic times, can be neglected for the  
77 short time solution. Because the potential frequencies are low enough compared to  
78 the plasma frequency, the Laplace equation reduces to the quasineutrality condition,  
79 i.e. the equality of electron and ion density perturbations. The small time equilibrium  
80 distribution function of the ions is obtained from the electron distribution:

$$81 \quad f_0^i = n_0(x) F_M^i \exp[e\phi_0(x, y - V_* t, z)/T_e], \quad (3)$$

82 where  $F_M^i$  is the Maxwell distribution of the parallel ion velocities. The integral  
83 over the perpendicular velocity was already performed since the dependence of the  
84 gyro-averaged potential on the Larmor radius is small at the wavelengths considered  
85 here. It can easily be checked that this function is a small time (smaller than the  
86 characteristic times of the last two terms in Eq. (1)) solution of the ion equation (1)  
87 if  $V_*$  is the diamagnetic velocity

$$88 \quad V_* = -\frac{T_e}{eB} \frac{1}{n_0} \frac{dn_0}{dx} = \frac{T_e}{eBL_n} = \frac{c_s \rho_s}{L_n}, \quad (4)$$

89 where  $c_s = \sqrt{T_e/m_i}$ ,  $\rho_s = c_s/\Omega_i$ , and  $\Omega_i = eB/m_i$ .

## 2.2. PERTURBATION OF THE BACKGROUND POTENTIAL

90 The change of the potential with  $\delta\tilde{\phi} = \varphi(z) \exp(ik_x x + ik_y y - i\omega t)$  leads to a  
91 variation of the distribution functions of both electrons and ions. Besides the adia-  
92 batic response obtained simply by replacing  $\phi_0 \rightarrow \phi_0 + \delta\tilde{\phi}$  in the equilibrium expres-  
93 sions, a new term  $h$  appears in the distribution functions:

$$94 \quad f_t^\alpha = f_1^\alpha + h^\alpha, \quad f_1^\alpha = n_0(x) F_M^\alpha \exp\left[e\left(\phi_0 + \delta\tilde{\phi}\right)/T_e\right], \quad (5)$$

95 where  $\alpha = e, i$  and  $h$  is the non-adiabatic term. It is useful at this point to rewrite Eq.  
96 (1) as  $\mathcal{O}^\alpha[\phi] f^\alpha = \mathcal{C}^\alpha$ , where the operator  $\mathcal{O}^\alpha[\phi]$  is the derivative along trajectories in  
97 the potential  $\phi$ , defined by:

$$98 \quad \mathcal{O}^\alpha[\phi] \equiv \partial_t - \frac{\nabla\phi \times \mathbf{b}}{B} \cdot \nabla + v_z \partial_z - \frac{q_\alpha}{m_\alpha} \partial_z \phi \frac{\partial}{\partial v_z}. \quad (6)$$

99 Expanding in the first order in the potential perturbation, we are left with:

$$100 \quad \mathcal{O}^\alpha[\phi_0 + \delta\tilde{\phi}] \left( f_0^\alpha (1 + e\delta\tilde{\phi}/T_e) + h^\alpha \right) = C^\alpha . \quad (7)$$

101 In the following, we shall evaluate this expression for electrons and ions separately.

### 2.3. ELECTRON RESPONSE

102 We need to consider two electron subsystems: trapped (due to the confining  
103 effect of the magnetic mirrors) and untrapped populations. In between the magnetic  
104 mirrors, i.e. for  $0 < |z| < L$ , where both species exist, the equilibrium densities are  
105 denoted by  $n_{0te}$  and, respectively,  $n_{0ue}$ , with  $n_{0te} + n_{0ue} = n_0$ . Here, we define the  
106 trapped electron fraction  $\delta = n_{0te}/n_0 < 1$ . Outside the magnetic mirrors, i.e. for  
107  $L < |z| < L'$ , there are only untrapped electrons having density  $n_0$ .

108 In the case of trapped electrons, we employ the Krook model for the colli-  
109 sion term [9, 10]: it describes the relaxation of the total distribution function to  
110 the adiabatic part with a velocity-dependent characteristic time  $\nu(\mathbf{v})^{-1}$ , thus  $\mathcal{C}^{te} =$   
111  $-\nu_e(\mathbf{v}) (f_t^{te} - f_1^{te}) = -\nu_e(\mathbf{v}) h^{te}$ , where the superscript "te" stands for the trapped  
112 electron population. Eq. (7) becomes, to first order in the perturbations:

$$113 \quad \mathcal{O}^{te}[\phi_0] h^{te} + \nu_e(\mathbf{v}) h^{te} = \frac{ef_0}{T_e} [T_{\delta\phi}^e + T_{\phi_0}^e] \delta\tilde{\phi} , \quad (8)$$

where;

$$T_{\delta\phi}^e = i\omega + i \frac{T_e}{eB} \frac{\partial_x [n_0 F_M^e]}{n_0 F_M^e} k_y \equiv i(\omega - \omega_e^*), \quad (9a)$$

$$T_{\phi_0}^e = \frac{\partial_y \phi_0}{B} \frac{\partial_x n_0}{n_0} \frac{\eta_e}{2} \left( -3 + \frac{m_e \mathbf{v}^2}{T_e} \right) , \quad (9b)$$

114 with  $\eta_e = L_n/L_{T_e}$ . The solution obtained by integrating Eq. (8) along the straight  
115 zero order electron trajectories between the two mirrors,  $z(\tau) = z + v_z(\tau - t)$ :

$$116 \quad h^{te} = f_0^{te} e^{i\mathbf{k}_\perp \cdot \mathbf{x}_\perp(t) - i\omega t} \int_{-\infty}^t d\tau [T_{\delta\phi}^e + T_{\phi_0}^e] e^{-i(\omega + i\nu_e)(\tau - t)} \frac{e\varphi(z(\tau))}{T_e} . \quad (10)$$

117 The  $T_{\phi_0}^e$  contribution vanishes upon averaging over the statistical realizations  
118 of the background turbulence, as  $\langle \varphi_0 \rangle = 0$ . The trapped electrons undergo a periodic  
119 motion between the two magnetic mirrors at  $z = \pm L$ , with a very fast bounce fre-  
120 quency  $\omega_{be} = v_z/2L$ . This allows us to average Eq. (10) over the bounce time scale:

$$121 \quad h^{te} = f_0^{te} \frac{e}{T_e} e^{i\mathbf{k}_\perp \cdot \mathbf{x}_\perp(t) - i\omega t} \int_{-\infty}^t d\tau e^{-i(\omega + i\nu_e)(\tau - t)} T_{\delta\phi} \bar{\varphi} , \quad (11)$$

123 where  $\bar{\varphi} = \frac{1}{2L} \int_{-L}^L dz' \varphi(z')$ . Performing first the time integral, then the velocity  
124 integral and finally assembling together the adiabatic and non-adiabatic parts of the

125 trapped electron density perturbations, we arrive at:

$$126 \quad \delta n_{te} = n_{0te} e^{i\mathbf{k}_\perp \cdot \mathbf{x}_\perp(t) - i\omega t} \frac{e}{T_e} \left( \varphi - \overline{\varphi} \left\langle \frac{\omega - \omega_e^*}{\omega + i\nu_e} \right\rangle_v \right), \quad (12)$$

127 where the notation  $\langle \dots \rangle_v$  indicates the integration over the velocity space with the  
 128 Maxwellian function. The imaginary part of the last term, which involves the elec-  
 129 tron collisionality, is the origin of the DTEM instability. Using the approximation  
 130  $\nu_e(\mathbf{v}) = \nu v_{th,e}^3 / (\epsilon |\mathbf{v}|^3)$  [11], together with the expressions of  $\omega_e^*$  in Eq. (9a) and that  
 131 of the Maxwellian function in Eq.(2) we evaluate the integral numerically, using the  
 132 Simpson rule. A study of the integral's behaviour as a function of collisionality can  
 133 be found in [15].

134 Collisions are not important for the untrapped electrons and their density per-  
 135 turbation is considered adiabatic, as in [9, 10]:

$$136 \quad \delta n_{ue} = n_{0ue} e^{i\mathbf{k}_\perp \cdot \mathbf{x}_\perp(t) - i\omega t} \frac{e\varphi}{T_e}. \quad (13)$$

137 Trajectory eddying is negligible for both electron populations due to their fast parallel  
 138 decorrelation.

#### 2.4. ION RESPONSE

139 For the collisionless ions a similar treatment to the one presented above leads  
 140 to the following expression for the linearized Eq. (7):

$$141 \quad \mathcal{O}^i[\phi_0] h^i = \frac{ef_0^i}{T_e} e^{i\mathbf{k}_\perp \cdot \mathbf{x}_\perp(t) - i\omega t} [T_{\delta\phi}^i + T_{\phi_0}^i] \varphi(z), \quad (14)$$

where:

$$T_{\delta\phi}^i = i\omega - iV_* k_y - \left( 1 + \frac{T_e}{T_i} \right) v_z \partial_z + i\rho_s^2 k_\perp^2 \omega, \quad (15a)$$

$$T_{\phi_0}^i = -\frac{e}{T_e} v_z \left( 1 + \frac{T_e}{T_i} \right) \partial_z \phi_0. \quad (15b)$$

142 In order to find the solution for the distribution function  $h^i(\mathbf{x}_\perp, z; v_z; t)$ , we  
 143 take into account that the operator  $\mathcal{O}^i[\phi_0]$  is the derivative along the ion trajectories  
 144 in the background field  $\phi_0$ , which are given by  $d\tilde{\mathbf{x}}_\perp/d\tau = -\nabla\phi_0(\tilde{\mathbf{x}}_\perp(\tau)) \times \mathbf{e}_z/B$ ,  
 145  $z(\tau) = z + v_z(\tau - t)$ . They are calculated backwards in time with the the boundary  
 146 condition  $\tilde{\mathbf{x}}_\perp(\tau = t) = \mathbf{x}_\perp$ . In order to obtain the

$$147 \quad h^i = \frac{ef_0^i}{T_e} e^{i\mathbf{k}_\perp \cdot \mathbf{x}_\perp - i\omega t} \int_{-\infty}^t d\tau [T_{\delta\phi}^i + T_{\phi_0}^i] \varphi(z(\tau)) e^{i\mathbf{k}_\perp \cdot (\tilde{\mathbf{x}}_\perp(\tau) - \mathbf{x}_\perp) - i\omega(\tau - t)}. \quad (16)$$

148 Due to the fact that  $v_{Ti}/(\omega L') \ll 1$  we may keep only the first term in the Taylor  
 149 expansion of  $\varphi(z(\tau))$ , which allows for an easy evaluation of the parallel velocity in-

150 tegrals. The  $T_{\phi_0}^i$  term contribution vanishes as the  $z$ -derivatives of  $\phi_0$  do not correlate  
 151 with the perpendicular displacements, and we are left with:

$$\delta n_i = n_0 \frac{e}{T_e} e^{i\mathbf{k}_\perp \cdot \mathbf{x}_\perp(t) - i\omega t} \left[ \omega - V_* k_y - \left( 1 + \frac{T_e}{T_i} \right) v_{T_i}^2 \partial_z^2 \partial_\omega + \rho_s^2 k_\perp^2 \omega \right] \varphi(z) \Pi^i(\omega), \quad (17)$$

152 where the ion propagator involves the average over the stochastic trajectories in the  
 153 background field:  
 154

$$\Pi^i(\omega) = i \int_{-\infty}^t d\tau e^{-i\omega(\tau-t)} \left\langle e^{i\mathbf{k}_\perp \cdot (\bar{\mathbf{x}}_\perp(\tau) - \mathbf{x}_\perp)} \right\rangle \quad (18)$$

## 2.5. DISPERSION RELATION

156 Taking into account Eqs. (12, 13, 17), the quasineutrality condition  $\delta n_{te} +$   
 157  $\delta n_{ue} = \delta n_i$  becomes:

$$-\delta \bar{\varphi} \left\langle \frac{\omega - \omega_e^*}{\omega + i\nu_e} \right\rangle_v = \left[ (1 + \rho_s^2 k_\perp^2) \omega - V_* k_y - \left( 1 + \frac{T_e}{T_i} \right) v_{T_i}^2 \partial_z^2 \partial_\omega \right] \varphi(z) \Pi^i(\omega). \quad (19)$$

158 Following [9, 10], we rearrange the previous equation as:  
 159

$$A(\omega) \varphi(z) - B(\omega) \varphi''(z) = C(\omega) \int_{-L}^L dz' \varphi(z'), \quad (20)$$

where:

$$A(\omega) = \left[ \frac{V_* k_y}{\omega} - (1 + \rho_s^2 k_\perp^2) \right] \cdot (-\omega) \Pi^i(\omega),$$

$$B(\omega) = \left( 1 + \frac{T_e}{T_i} \right) c_s^2 \frac{\partial}{\partial \omega} \Pi^i(\omega), \quad C(\omega) = -\frac{\delta}{2L} \left\langle \frac{\omega - \omega_e^*}{\omega + i\nu_e} \right\rangle_v. \quad (21)$$

161 Eqs. (21) are in agreement with the corresponding expressions found in Refs. [9, 10],  
 162 in the case of quiescent plasmas where  $\Pi^i = -1/\omega$ . Our treatment additionally gener-  
 163 erates a finite Larmor radius correction ( $1 + \rho_s^2 k_\perp^2$ ) and a temperature ratio correction  
 164 ( $1 + T_e/T_i$ ) to the ion terms.

165 Outside the magnetic mirrors there are no trapped electrons and thus their con-  
 166 tribution to the right hand side of Eq. (20) vanishes. We may write the equation valid  
 167 on the entire interval  $-L' < z < L'$  as:

$$A(\omega) \varphi(z) - B(\omega) \varphi''(z) = C(\omega) \int_{-L}^L dz' \varphi(z') \text{rect}(z; L) \quad (22)$$

169 where the rectangular function is defined as  $\text{rect}(z; L) = \theta(z - L) - \theta(z + L)$ , with  
 170  $\theta(z)$  the Heaviside step function.

## 2.6. EXACT SOLUTION

171 Usual treatments of the DTEM instability involve a harmonic expansion of the  
 172 test mode [9, 10, 15, 16]. In the following we present the exact solution of Eq. (22),  
 173 which allows the derivation of an explicit dispersion relation. By using the notations  
 174  $\lambda^2 = A/B$ ,  $\chi = -C/B$ , we may rewrite the quasineutrality condition, Eq. (22), in a  
 175 simplified form:

$$176 \quad \varphi''(z) - \lambda^2 \varphi(z) = \chi \int_{-L}^L dz' \varphi(z') \text{rect}(z; L) \quad (23)$$

177 In order for the bounce averaged potential to be nonvanishing, we expect even so-  
 178 lutions  $\varphi(z) = \varphi(-z)$  and thus we restrict our attention to the interval  $z \in [0, L']$ .  
 179 At the origin  $z = 0$  we choose for simplicity the normalization  $\varphi_1(0) = 1$ , as the  
 180 equation is homogeneous. By imposing  $\varphi'_1(0) = 0$  we ensure the evenness of the  
 181 solution. At  $z = L$  the rectangular function on right hand side has a finite discontinu-  
 182 ity, which preserves the continuity of the function itself and that of its first derivative  
 183 at this point, thus  $\varphi(L_-) = \varphi(L_+)$  and  $\varphi'(L_-) = \varphi'(L_+)$ . We obtain the following  
 184 expression for the function  $\varphi(z)$ :

$$185 \quad \varphi(z) = \begin{cases} \frac{\lambda (\lambda^2 + 2L\chi) \cosh(\lambda z) - 2\chi \sinh(\lambda L)}{\lambda (\lambda^2 + 2L\chi) - 2\chi \sinh(\lambda L)} & 0 \leq z \leq L \\ \frac{\lambda (\lambda^2 + 2L\chi) \cosh(\lambda z) - \chi [\sinh(2\lambda L - \lambda z) + \sinh(\lambda z)]}{\lambda (\lambda^2 + 2L\chi) - 2\chi \sinh(\lambda L)} & L < z \leq L' \end{cases} \quad (24)$$

186 The condition  $\varphi'(L') = 0$ , consistent with the above mentioned harmonic ex-  
 187 pansion, leads to the dispersion relation:

$$188 \quad \lambda (\lambda^2 + 2L\chi) \sinh(\lambda L') + \chi [\cosh(2\lambda L - \lambda L') - \cosh(\lambda L')] = 0. \quad (25)$$

189 For simplicity we will restrict ourselves to the case  $L' = 2L$ , where the previous  
 190 equation reduces to:

$$191 \quad \frac{1}{\lambda L'} \tanh\left(\frac{\lambda L'}{2}\right) = 1 + \frac{\lambda^2}{\chi L'}. \quad (26)$$

## 2.7. RESULTS AND DISCUSSIONS

192 We have analyzed Eq. (26) in the case of quiescent plasmas, quasilinear and  
 193 nonlinear regimes. In the following we use dimensionless quantities normalized us-  
 194 ing the units of length  $\rho_s$  and time  $L_n/c_s$ , i.e.  $k_i \rightarrow k_i \rho_s$ ,  $\omega \rightarrow \omega L_n/c_s$ ,  $\Pi^i \rightarrow$   
 195  $\Pi^i c_s/L_n$ ,  $\nu \rightarrow \nu L_n/c_s$ ,  $D_i \rightarrow D_i L_n/(\rho_s^2 c_s)$ . The numerical values of the relevant  
 196 quantities are:  $L' = 2L = 2m$ ,  $T_i/T_e = 1/3$ ,  $L_n = L_{T_e} = 10cm$ ,  $\epsilon = 0.63$ .

197 Typical results in the case of quiescent plasmas with  $\phi_0 = 0$  are presented in  
 198 Fig. (1). Unstable modes are present in the low  $k_y$  and high  $k_y$  regions. The fre-

199 quencies increase with the increase of trapped electron fraction  $\delta$  and are weakly  
 200 influenced by the electron collision frequency  $\nu$ . The growth rates are increasing  
 201 functions of both  $\delta$  and  $\nu$ , which shows that DTEMs are unstable due to the com-  
 202 bined action of electron trapping by the magnetic mirrors and electron collisions.

203 In the weak turbulence regime, the Gaussian distribution of ion displacements  
 204 leads to ion trajectory diffusion. The propagator of Eq. (18) becomes in this case  
 205  $\Pi^i = -1/(\omega + ik_i^2 D_i)$ , where the diffusion coefficient is defined as usual by  $D_i =$   
 206  $\langle [x_i(\tau) - x_i(t)]^2 \rangle / (t - \tau)$ . Fig. (2) shows that ion diffusion determines the damp-  
 207 ing of high  $k$  modes, in accordance with the well known results of Dupree. As a  
 208 result, the increase of the turbulence amplitude is accompanied by the increase of its  
 209 correlation length.

210 An increase in the amplitude of the stochastic potential causes deviations from  
 211 the Gaussian distribution of the ion trajectories, due to the appearance of trapped  
 212 trajectories leading to quasicohherent structures [12, 13]. Ion trajectories are of two  
 213 types with different motions. The trapped trajectories have frozen mean square dis-  
 214 placements  $S_i$ , while the free trajectories have a Gaussian distribution with diffusive  
 215 evolution. The propagator is modified as [12]  $\Pi^i = -e^{-k_i^2 S_i/2} / (\omega + ik_i^2 D_i)$ .

216 The exponential factor may be absorbed into an effective,  $k$ -dependent, trapped  
 217 electron fraction  $\delta_{eff}(\mathbf{k}) = \delta e^{k_i^2 S_i/2}$ . Being an increasing function of  $k$ , it has a  
 218 destabilizing influence on high  $k$  modes, which is opposed by the damping due to  
 219 ion diffusion. The competition of the two effects leads to the appearance of the  
 220 maximum in the growth rates.

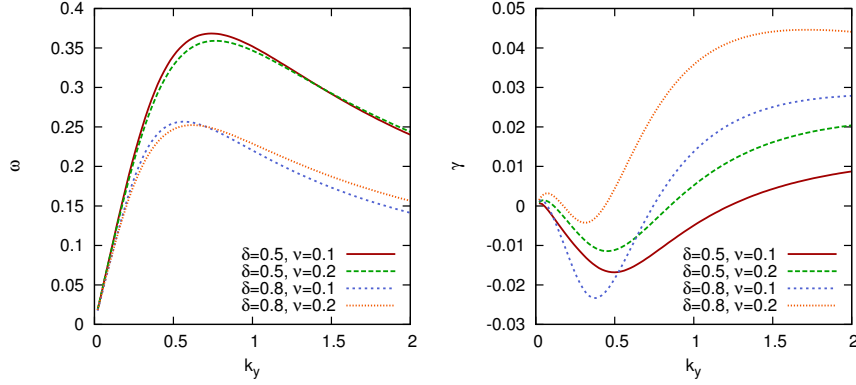
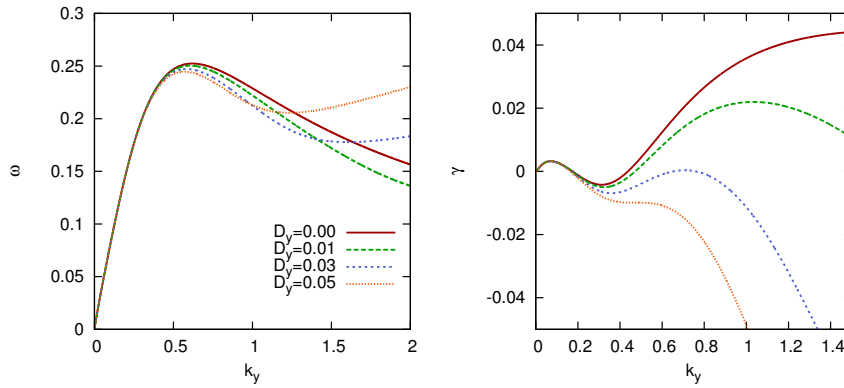
221 The increase of  $\delta_{eff}$  due to ion trajectory structures also determines the de-  
 222 crease of the frequencies. As seen in Fig. (3), DTEMs that are damped by diffusion  
 223 grow back due to trajectory structures. Unstable modes appear in turbulent plasmas  
 224 in the range of wave numbers  $k_x, k_y \sim 0.5$ .

### 3. CONCLUSIONS

225 We have analyzed in a plasma slab model the influence of the background tur-  
 226 bulence on the characteristics of the dissipative trapped electron instability. We have  
 227 deduced the dispersion relation for test modes, dependent on the statistical proper-  
 228 ties of the background stochastic potential. We have shown that the turbulence does  
 229 not change the structure of the dispersion relation of Eq. (23), but it influences the  
 230 functions  $A$ ,  $B$  and  $C$ . We have found an exact solution of the dispersion relation.

231 The background turbulence influences the DTEMS through the ion response.  
 232 The stochastic potential  $\phi_0$  determines the diffusion of ion trajectories and, at larger  
 233 amplitudes, the formation of ion trajectory structures due to ion eddying.

234 The diffusion has a damping effect on the large  $k_y$  modes, which is accompa-

Fig. 1 – Frequencies and growth rates in the quiescent case,  $k_x = 0$ .Fig. 2 – The effect of ion trajectory diffusion on the frequencies and growth rates in the quasilinear case,  $\delta = 0.8$ ,  $\nu = 0.2$ ,  $k_x = 0$ .

235 nied by the increase of the frequencies. At values of the order  $D_i \sim 0.2\rho_s V_*$ , the  
 236 DTEMs are damped except for  $k_y \rho_s < 0.1$ .

237 Ion trajectory trapping determines the increase of the effective ratio of the elec-  
 238 trons trapped by the magnetic mirrors, which leads to the increase of the growth rates.  
 239 In this nonlinear regime, at structure sizes  $S_i \sim 2 \div 3$ , the ion eddying destabilizing  
 240 effect overcomes the diffusive damping and leads to large growth rates, of the order  
 241 of  $\gamma$  in the absence of turbulence.

242 A self consistent coupled test particle and test mode study similar to [17] will  
 243 be developed in a future work. The effective interaction of the physical processes

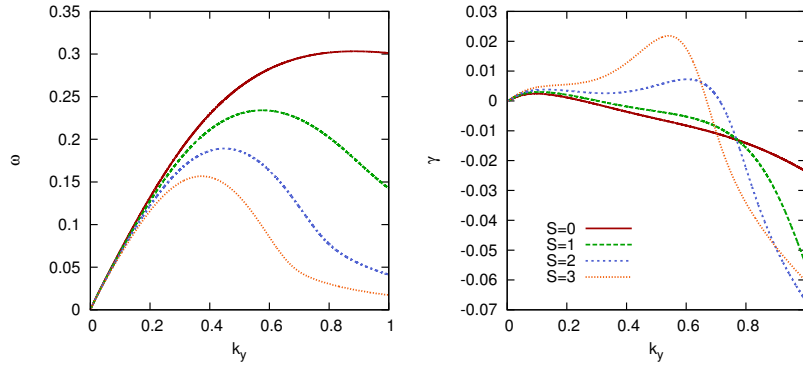


Fig. 3 – Frequencies and growth rates in the weakly nonlinear case,  $\delta = 0.5$ ,  $\nu = 0.2$ ,  $k_x = 0.5$ ,  $D_y = 0.05$ ,  $S_x = S_y = S$ .

244 found here and the evolution of DTEM turbulence will be analyzed.

245 *Acknowledgments.* This work has been carried out within the framework of the EUROfusion  
 246 Consortium and has received funding from the Euratom research and training programme 2014-2018  
 247 under grant agreement No 633053. The views and opinions expressed herein do not necessarily reflect  
 248 those of the European Commission.

#### REFERENCES

- 249 1. W. Horton, Rev. Mod. Phys. **71**, 735 (1999).  
 250 2. X. Garbet, Y. Idomura, L. Villard, and T. H. Watanabe, Nucl. Fusion **50**, 043002 (2010).  
 251 3. G. R. Tynan, A. Fujisawa, and G. McKee, Plasma Phys. Controlled Fusion **51**, 113001 (2009).  
 252 4. P. H. Diamond, A. Hasegawa, and K. Kima, Plasma Phys. Controlled Fusion **53**, 124001 (2011).  
 253 5. R. E. Waltz, Phys. Fluids **28**, 577 (1985).  
 254 6. G. G. Craddock, A. E. Koniges, J. A. Crotinger, P. H. Diamond, D. E. Newman, and P. W. Terry,  
 255 Phys. Plasmas **1**, 1877 (1994).  
 256 7. J. Lang, Y. Chen, S. E. Parker, Phys. Plasmas **14**, 082315 (2007).  
 257 8. J. Anderson, H. Nordman, R. Singh, J. Weiland, Plasma Phys. Control. Fusion **48** (2006) 651-661  
 258 9. S. C. Prager, A. K. Sen, T. C. Marshall, Phys. Rev. Lett., Vol. 33, No. 12, September 1974.  
 259 10. S. C. Prager, T. C. Marshall, A. K. Sen, Plasma Phys., Vol. 17, pp. 785-797 (1975)  
 260 11. B. B. Kadomsev, O. P. Pogutse, Soviet Phys. Dokl. **14**, 470 (1969)  
 261 12. M. Vlad, Phys. Rev. E **87**, 053105 (2013)  
 262 13. M. Vlad, F. Spineanu, Phys. Rev. E **70**, 056304 (2004).  
 263 14. M. Vlad, F. Spineanu, New J. Phys. **19**, 025014 (2017)  
 264 15. D. P. Dixon, T. C. Marshall, A.K. Sen, Plasma Phys., Vol. 20, pp. 189-196 (1978)  
 265 16. C. A. Primmerman, L. M. Lidsky, P. A. Politzer, Phys. Rev. Lett., Vol. 33, No. 16 (1974)  
 266 17. M. Vlad, F. Spineanu, V. V. Baran, in preparation.  
 267 18. M. Vlad, F. Spineanu, J. H. Misguich, and R. Balescu, Phys. Rev. E **58**, 7359 (1998).